Mode Coupling Between Dielectric and Semiconductor Planar Waveguides

T. E. BATCHMAN, MEMBER, IEEE, AND GLEN M. MC WRIGHT, STUDENT MEMBER, IEEE

Abstract—**Computer modeling studies on four-layer silicon-clad planar dielectric waveguides indicate that the attenuation and mode index behave as exponentially damped sinusoids when the silicon thickness is increased. This effect can be explained as a periodic coupling between the guided modes of the lossless structure and the lossy modes supported by the high refractive index silicon. Furthermore, the attenuation and mode index are significantly altered by conductivity changes in the silicon. An amplitude modulator and phase modulator have been proposed using these results. Predicted high attenuations in the device may be reduced significantly with a silicon dioxide buffer layer.**

I. Introduction

THERE has been considerable interest in metal-clad optical waveguides since they are used for electrooptic and magnetooptic devices [1]-[10]. It has also been suggested that metal-clad optical guides be used as polarizers for integrated optics [11]. Semiconductor-clad or positive-permittivity metal-clad waveguides have been analyzed more recently, and measurements have confirmed the predicted characteristics of such guides [12], [13]. Both the metal- and semiconductor-clad guides are extremely lossy in the visible region, especially when the waveguide thickness is thin enough to preclude all but the lowest order TE or TM modes from propagation. Partly because of these high losses, semiconductor-clad waveguides have found few applications in integrated optical devices, although it has been suggested by Lee *et al.* [14] that such waveguides be used for optical control of millimeter-wave propagation in dielectric waveguides. The calculations presented here will suggest two applications for these clad waveguides in the optical propagation region.

The permittivity of a lossy material is given by

$$\hat{\epsilon}_r = \epsilon' - j\epsilon'' = \epsilon' - j\frac{\sigma}{\omega\epsilon_o} \tag{1}$$

where σ is the conductivity of the metal at frequency ω. The permittivity can also be expressed in terms of the refractive index as

$$\hat{n} = \hat{\epsilon}^{1/2} = n - jk \tag{2}$$

where n and k are the real and imaginary parts of the refractive index, respectively. Although values for these parameters are sometimes hard to find, they are usually available for bulk semiconductors [15]. Values for amorphous and polycrystalline films formed by vacuum deposition are not as readily available [16], [17] since they often depend on the deposition technique used. The complex nature of the material permittivity makes the analysis of even planar waveguide structures difficult, and thus, elaborate computer solution techniques must be employed. Although Lee *et al.* [14] have shown that both the real and imaginary parts of the permittivity vary with incident light intensity, the variation in the real part can be shown to be relatively small compared to the imaginary part. It has thus been assumed that if light is incident on the semiconductor cladding, then the major change will be in the conductivity, which is given by

$$\sigma = \sigma_o + e\,\Delta n(\mu_e + \mu_h) \tag{3}$$

where μ_e and μ_h are the electron and hole mobilites, respectively. The dark conductivity σ_o is then changed by the creation of a number of hole-electron pairs $\Delta n = \Delta p$. The total conductivity, and consequently, complex permittivity of any semiconductor can thus be changed by the creation of hole-electron pairs.

During an investigation of planar waveguide structures which utilize this externally induced permittivity change, it was discovered that these structures exhibit periodic coupling between modes in the dielectric waveguide and a semiconductor cladding. It was further noted that changes in the conductivity of this lossy semiconductor cladding produced relatively large changes in the attenuation and phase constants of the propagating mode in the dielectric waveguide. The periodic coupling and the resulting modulation effects are discussed in detail in the following paragraphs.

II. Theory and Notation

The four-layer planar waveguide structure under consideration is shown in Fig. 1 where the guided light is propagating in the z-direction in the dielectric (N_3), and it is assumed there is no variation in the y-direction. All materials are lossless except for the semiconductor (N_2). The dispersion relations for this structure are well known, and two methods of solution for the complex mode propagation constant ($\alpha + j\beta$) have been described previously [8], [18].

In the first technique, the operator selects initial guesses for α and β and convergence factors for error estimation. The computer then uses a random walk technique to calculate values for α and β satisfying the dispersion relation for the structure of interest [8]. In the second method, matrices are created for each layer based on given constraints and a characteristic matrix for the entire structure is obtained. Solving

Manuscript received September 2, 1981; revised October 2, 1981. This work was supported by the NASA Langley Research Center.

The authors are with the Department of Electrical Engineering, University of Virginia, Charlottesville, VA 22901.

0018-9480/82/0400-0628$00.75

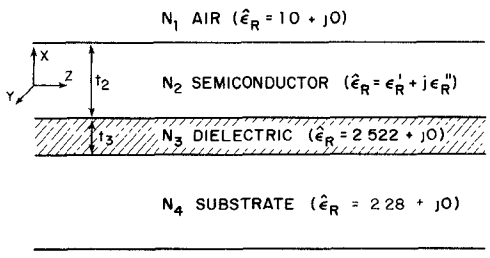

Fig. 1. Four-layer planar waveguide structure.

for the eigenvalues yields the complex mode propagation constant. Calculations presented here were originally obtained using the dispersion relation approach and later confirmed with the eigenvalue method [18].

The waveguide consists of a semi-infinite glass substrate, a dielectric core of thickness 1 μm, a semiconductor cladding varying from 0.01 to 10 μm in thickness, and a semi-infinite layer of air. A free-space wavelength of 632.8 nm was assumed, and all material parameters shown in Fig. 1 are for this wavelength. The three most common semiconductors, silicon, gallium arsenide, and germanium, were used as the cladding layer, and relative permittivity values are summarized in Table I. Bulk values have been used where data were not available for thin films. As previously noted, the refractive index of thin amorphous semiconductor films depends on the method of deposition and any impurities deliberately or accidently added to the semiconductor [19], [20]. Measurements of deposited films will thus be required before experimental results can be compared to the predictions presented here.

III. Comparison of Cladding Materials

Silicon was selected as the first semiconductor cladding material to be investigated, and the attenuation and phase constant curves of Figs. 2 and 3 were generated by varying the cladding thickness from 0.01 to 10 μm. (The phase constant β has been normalized by $k_o = 2\pi/\lambda_o$ so that all curves show the mode index.) All other parameters were held constant in these calculations and results were confirmed by using both computer solution techniques [8], [18]. It was initially expected that decreasing the lossy cladding thickness to 0.01 μm would reduce the attenuation to zero in a well-behaved manner; however; the results were not as expected below a silicon thickness of 1.0 μm. The curves are similar to exponentially damped sinusoids, with extreme values of the mode index (β/k_o) curves corresponding to the median values (maximum slope) in the attenuation (α) curves. Extreme values of the α curve correspond to median values in the β/k_o curves and the oscillations in both curves approach the median value at 1.0 μm.

Since the period of these oscillations (0.08-0.09 μm) is not a fraction of the wavelength of light in the dielectric (λ_d = 0.3985 μm), it must be related to either the waveguide structure or the properties of the semiconductor cladding. Gallium arsenide, which has a complex permittivity that is nearly the same as silicon, was used for the next series of calculations. The attenuation and phase characteristics were almost identical to those of silicon, and varying the dielectric waveguide thickness t_3 to 0.8 μm had little effect on the characteristics.

TABLE I
Semiconductor Parameters at λ = 632.8 nm

Material	Relative Permittivity ε'_r	Relative Permittivity ε''_r	Refractive Index n	Refractive Index k
Silicon*	16.76	1.75	4.1	0.213
Gallium Arsenide	14.3	1.21	3.79	0.16
Germanium*	14.43	19.54	4.4	2.22

* values for amorphous thin films

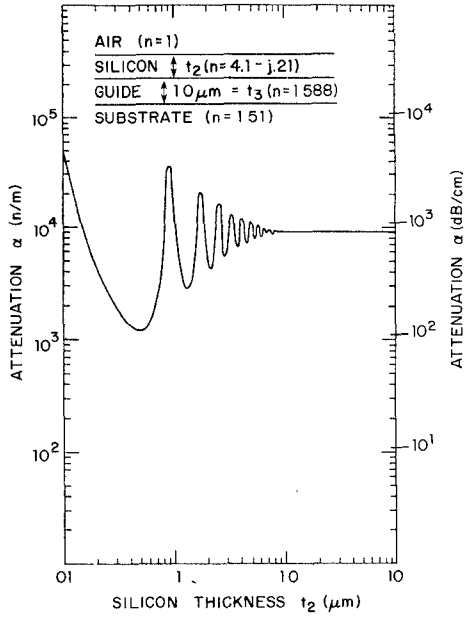

Fig. 2. Attenuation characteristics of silicon-clad waveguide (TE_0 mode, normal conductivity).

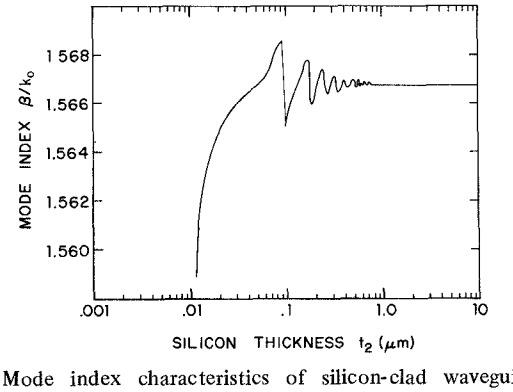

Fig. 3. Mode index characteristics of silicon-clad waveguide (TE_0 mode, normal conductivity).

The dielectric and glass layers were interchanged (i.e., glass substrate, GaAs, dielectric, air) and the rate of exponential decay increased, but the period remained constant.

As Table I indicates, the permittivity of germanium has a significantly larger imaginary part and would thus be expected to have the largest effect on the observed characteristics. Figs. 4 and 5 show that the larger conductivity of germanium nearly eliminates the damped oscillatory behavior in the thickness region of interest. The damping is so rapid that it is difficult to determine an oscillation period.

A similar effect had been noted by Heavens [21] and Strat-

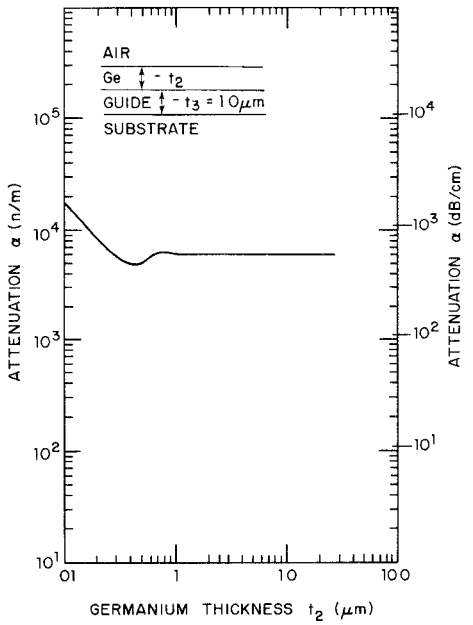

Fig. 4. Attenuation characteristics of germanium-clad waveguide.

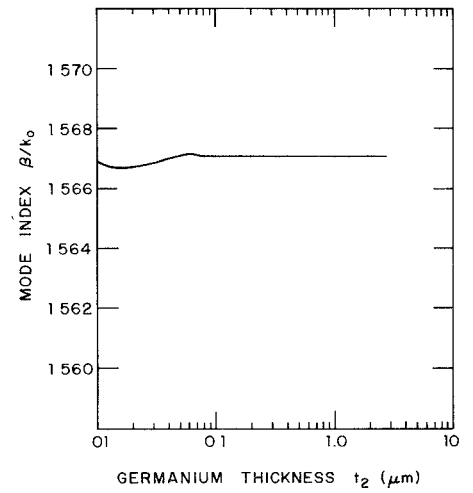

Fig. 5. Mode index characteristics of germanium-clad waveguide.

ton [22] for semiconductor and metal films, respectively. Heavens considers thin films of a material with $n = 2$ and k varying, and calculates the expected phase change on reflection of a normally incident wave on an air-film surface. For very small k, the phase change oscillates, while for large k, the phase changes very little until the film thickness approaches zero. Neither author makes use of this property or considers such materials as waveguide claddings. To better understand the oscillatory behavior, the electric and magnetic field distributions in the four-layer waveguide were examined at the local maxima and minima points on the attenuation versus silicon thickness curve. The real part of the TE_0 mode electric field profile in the transverse direction is shown for a cladding thickness $t_2 = 0.007$ μm (Fig. 6). Note that the profile is everywhere positive and not appreciably distorted from that for the TE_0 mode of a three-layer lossless dielectric waveguide.

For the first local minimum at $t_2 = 0.05$ μm, the field begins to oscillate and crosses the zero axis at the silicon-dielectric

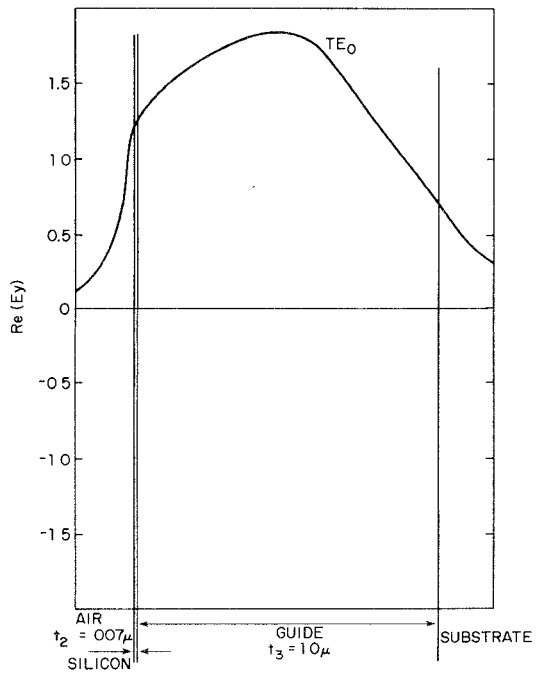

Fig. 6. Wave function profile, $t_{Si} = 0.007$ μm.

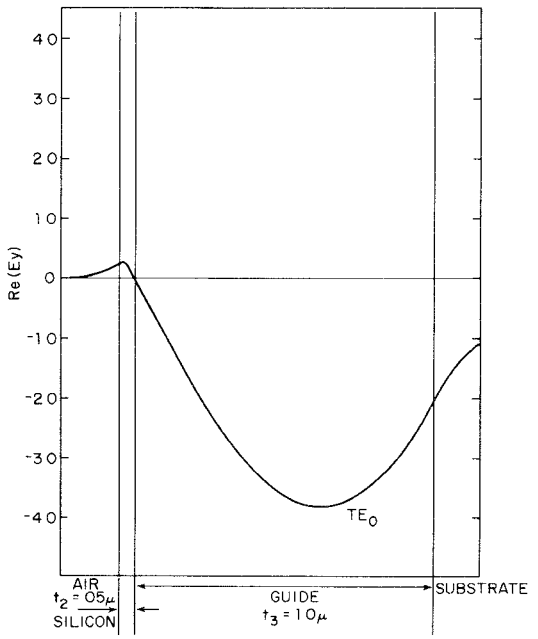

Fig. 7. Wave function profile, $t_{Si} = 0.05$ μm (local minimum).

interface (Fig. 7). For the local maximum at $t_2 = 0.09$ μm, the wave function profile has a sharp peak at the interface and oscillations continue (Fig. 8). Similar behavior is observed for the next local minimum and maximum pair ($t_2 = 0.13$ μm and $t_2 = 0.18$ μm, respectively). The field strength is effectively zero at the silicon-dielectric interface for the minimum and reaches a sharp peak at the interface for the maximum point on the attenuation curve.

As Figs. 9 and 10 indicate, this behavior continues for the next minimum and maximum pair ($t_2 = 0.22$ and 0.26 μm, respectively). It is now evident that the field in the silicon adds another $\frac{1}{4}$ cycle of oscillation between each maxima and

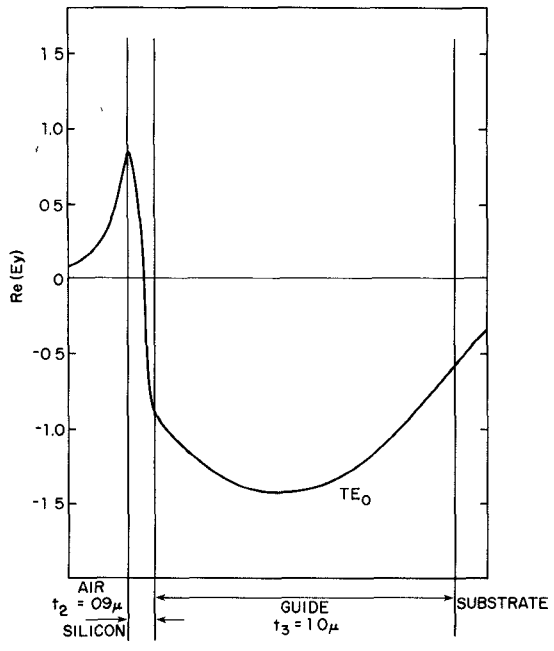

Fig. 8. Wave function profile, $t_{Si} = 0.09$ μm (local maximum).

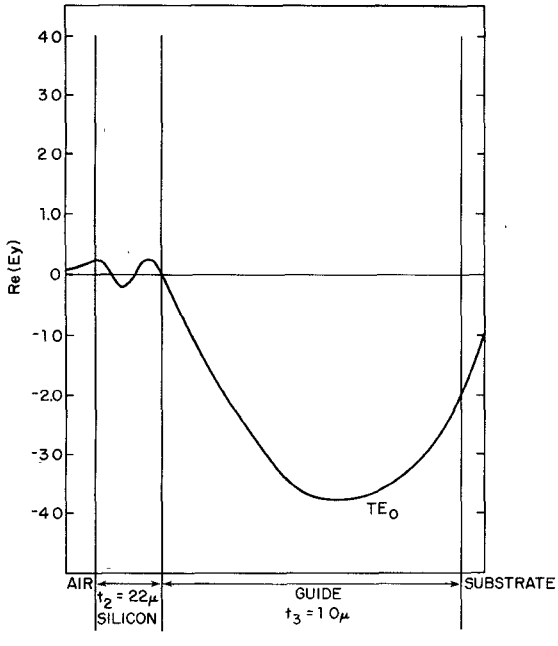

Fig. 9. Wave function profile, $t_{Si} = 0.22$ μm (local minimum).

minima, which suggests that as the silicon thickness increases, the energy from the dielectric waveguide couples into higher order modes in the silicon which now behaves as a lossy waveguide. Fig. 10 also exhibits the characteristic sharp peak at the interface but the field in the dielectric decays very rapidly, indicating almost complete energy transfer to the silicon. For the other maxima shown, there was still a sizable field in the dielectric waveguide, which suggests the local maxima and, likely, the minima values used for the field calculations were not the precise values. Additional calculations confirmed that a significant field again existed in the dielectric when t_2 was changed from 0.26 μm to 0.26 ± 0.005 μm.

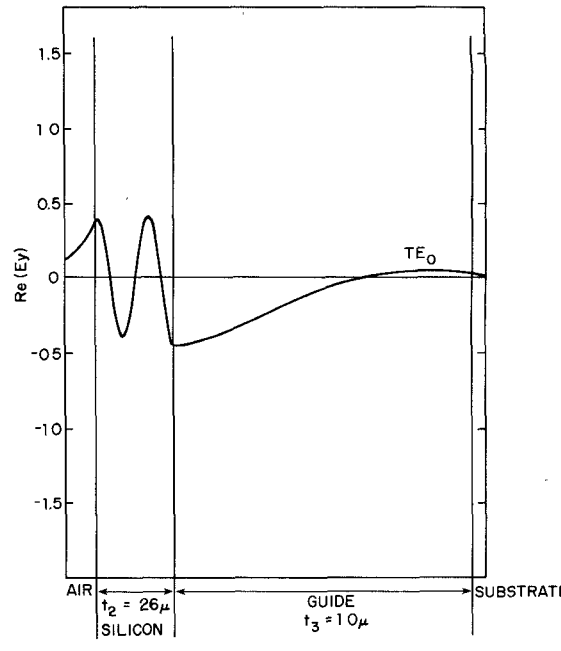

Fig. 10. Wave function profile, $t_{Si} = 0.26$ μm (local maximum).

It is evident from the field distributions that the presence of extremely thin films of silicon (<100 Å) has little effect on the dielectric waveguide; it behaves as a three-layer lossless structure (air-dielectric-substrate). For thicker silicon films, however, the TE_0 mode of the dielectric waveguide couples into the modes associated with the semiconductor film. As might be expected, the high refractive index silicon behaves as a lossy waveguide.

IV. Analysis of Coupling Characteristics

The results discussed above can be described as a periodic coupling between the guided mode (TE_0) in the dielectric and the lossy TE′ modes[1] of the semiconductor waveguide. This coupling has a profound effect on the attenuation and phase characteristics of the original four-layer waveguide. Since the field plots indicate successive coupling to higher order modes in the silicon layer, a partial structure consisting of a silicon guiding region surrounded by semi-infinite layers of air and dielectric was analyzed.

Figs. 11 and 12 show the mode index and attenuation constants for the first few low-order TE′ modes in the silicon waveguide. All modes are very lossy, and the attenuation increases for the higher order modes. In Fig. 11, note that a phase match condition between the TE′ modes of the partial structure (air-silicon-dielectric) and the TE_0 mode of the complete waveguide (Fig. 3) occurs at the cutoff thickness for successively higher order modes of the partial structure. The sharp peaks on the attenuation curve for the four-layer structure (Fig. 2) occur whenever the guided wave mode index matches that of one of the high loss TE_i' modes of the partial structure. The sharp nulls in the attenuation curve, indicating very low coupling efficiency, occur at thicknesses midway

[1] TE_i' denotes guided modes in the semiconductor and TE_i denotes guided modes in the dielectric.

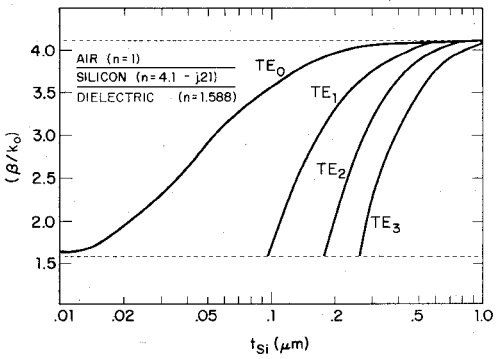

Fig. 11. Mode index characteristics of silicon waveguide.

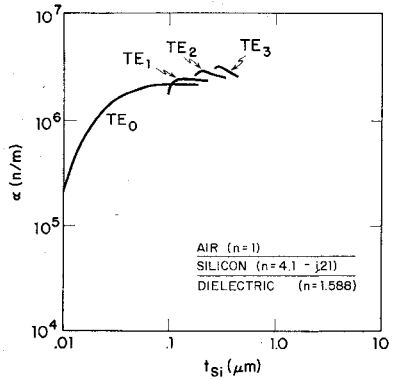

Fig. 12. Attenuation characteristics of silicon waveguide.

between the cutoff value of two adjacent lossy TE′ modes. Fig. 11 also indicates that the TE_0' mode in silicon does not cut off sharply as the higher order modes do. Lack of a well-defined cutoff is a characteristic usually associated with the TM_0 and surface wave modes [12]. The abrupt transitions on the mode index curve of the complete structure (Fig. 3) occur when the phase match condition is satisfied and the guided waves couple into successively higher order modes of the partial structure. These results are similar to the power transfer calculations for linearly tapered directional couplers [23]-[25] where the semiconductor is assumed to be lossless at the wavelength of interest.

Close examination of Fig. 2 indicates that the attenuation in the region of an oscillation minima is governed by an equation of the form

$$\alpha = K(1 - e^{-\alpha_i t_{2i}} \cos \omega t_{2_i}) \tag{3}$$

where

K = semi-infinite attenuation of the four-layer waveguide (i.e., when $t_2 \to \infty$),
α_i = attenuation (n/m) of the three-layer silicon waveguide at thickness t_{2_i},
t_{2_i} = thickness of the silicon at any point near a local minima (i) in the range $0.1 < t_2 < 1.0$ μm,
ω = period of the oscillation determined by the cutoff thickness of each TE′ mode.

For the silicon waveguide of Fig. 2, this equation becomes

$$\alpha = 9.1 \times 10^3 \left[1 - e^{-\alpha_i t_{2i}} \cos\left(\frac{2\pi \times 10^6}{0.085} t_{2_i}\right)\right] \text{n/m}. \tag{4}$$

The field plots and the analysis of the partial structure indicate, then, that the attenuation and mode index of the four-layer structure may be explained as a coupling between the basic TE_0 mode of the dielectric waveguide and the high-loss TE′ modes of the semiconductor guide. As more TE′ modes are excited, the effect on the TE_0 mode becomes negligible and the waveguide characteristics exponentially approach those of the three-layer structures previously analyzed [12], where the semiconductor layer is considered semi-infinite.

V. Applications

The imaginary portion of the relative permittivity of a semiconductor is a linear function of the conductivity and can thus be externally varied. Based on the observed attenuation and phase characteristics of germanium-clad waveguides (ϵ_r'' large), the conductivity of silicon was increased by 10, 25, and 50 percent to confirm that the amplitude of the oscillations decrease with increasing conductivity. The attenuation and phase oscillations both decrease in proportion to the increase in conductivity of the silicon layer. The calculated percentage change in attenuation and relative phase shift with conductivity as a parameter are shown in Figs. 13 and 14, respectively. Fig. 13 shows the percentage change in attenuation compared to the normal attenuation calculated with $\sigma = \sigma_o$ (dark conductivity). The curve crosses the horizontal axis when the attenuation is equal to that of the 10 μm silicon thickness structure. Fig. 14 shows the relative change in phase shift compared to the $\sigma = \sigma_o$ value, where the phase shift is given per millimeter of length of silicon in the z-direction. Both the attenuation and phase shift changes increase with increasing conductivity, and the percentage change increases as the silicon thickness approaches 0.1 μm. Both changes are large enough to be readily measurable and useful for device application.

One device utilizing these effects would be a waveguide amplitude or phase modulator. To amplitude modulate, a film of either silicon or gallium arsenide would be deposited on a dielectric waveguide transverse (y) to the direction of propagation (z). The thickness of the film would be determined by the type of modulator desired. For example, an amplitude modulator might be constructed with a silicon thickness of 0.05 or 0.13 μm (in the x-direction). The length of the modulator in the z-direction would likely be less than 1 mm. To modulate the light wave in the dielectric guide, the semiconductor conductivity could be varied by a variety of methods including heat, electric fields, or an incident incoherent light beam with photon energy above the bandgap of the silicon. In a similar manner, a phase modulator could be constructed by selecting the semiconductor thickness to produce maximum phase shift with conductivity change.

Since even relatively short sections of semiconductor-clad waveguides are lossy (1 mm length of Si at $t_2 = 0.05$ μm, $\alpha > 10$ dB), the attenuation must be reduced significantly for a practical device. Thin dielectric buffer layers are commonly used to lower the attenuation losses of metal-clad dielectric waveguides [26], [27]. These layers are placed between the dielectric core and the metal, and act as buffers to remove a large proportion of the field from the metal cladding. The effect of a silicon dioxide (SiO_2) buffer layer on the attenuation versus silicon thickness characteristics are investigated.

The results for silicon dioxide buffer layers of several different thicknesses and two different permittivities are shown

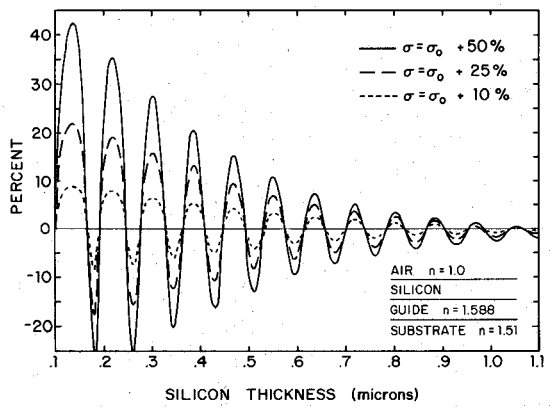

Fig. 13. Change in attenuation with relative change in conductivity (σ_O).

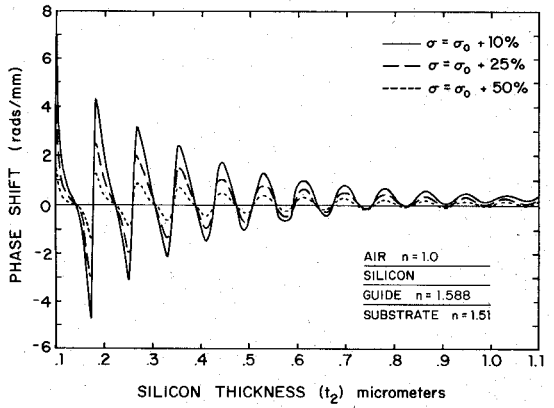

Fig. 14. Change in mode index with relative change in conductivity (σ_O).

in Figs. 15 and 16. Note that the familiar damped sinusoidal behavior is present and that the attenuation is reduced significantly. It was also found that the buffer layer increases the mode index slightly and decreases the amplitude of the oscillations, but the phase shift is still large enough to be useful for modulation.

In addition to the previously suggested tapered coupler [24], it may be possible to use the effect in a coupling or switching layer between two dielectric waveguides. If the semiconductor layer were sandwiched between two dielectric waveguides, the field coupling between the two dielectrics could be controlled by changing the conductivity of the semiconductor. The semiconductor film thickness would be selected to provide maximum field strength to the semiconductor and thus, the second waveguide. Increasing the semiconductor conductivity would then decrease the coupling between waveguides. A semiconductor film would also be applicable to fiber-to-waveguide couplers [28], [29] where the coupling could be varied through changes in the semiconductor conductivity.

VI. Conclusions

It has been shown that dielectric waveguides clad with lossy semiconductor films exhibit a damped periodic oscillation in their attenuation and phase characteristics. This is due to the periodic coupling between the lossy guided modes in the silicon film and the TE_0 mode in the dielectric waveguide. Suggested applications for this effect as modulators and waveguide switches have yet to be experimentally verified, and the practical application of such devices will depend upon how efficiently the semiconductor conductivity can be varied by an external source. Experimental devices are currently being constructed to verify the predicted effects.

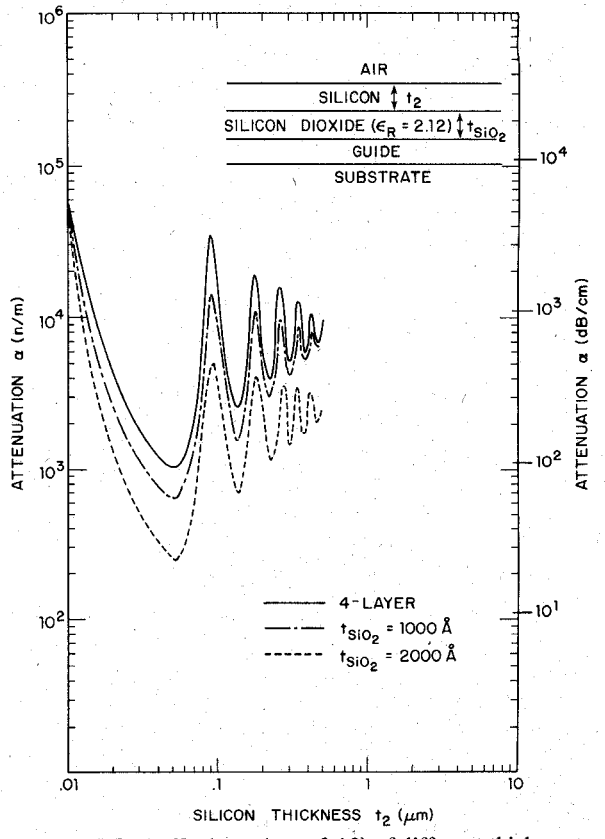

Fig. 15. SiO_2 buffer layer (ϵ_R = 2.12) of different thicknesses.

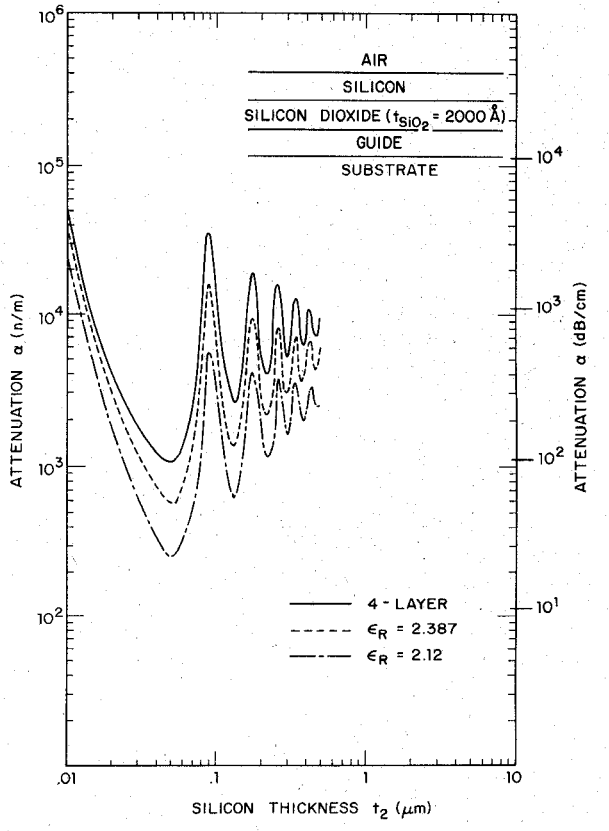

Fig. 16. SiO_2 buffer layer (t_{SiO_2} = 2000 Å) of different permittivities.

REFERENCES

[1] H. J. Fink, "Propagation of waves in optical waveguides with various dielectric and metal claddings," *IEEE J. Quantum Electron.*, vol. QE-12, pp. 365-367, June 1976.

[2] Y. Yamamoto, T. Kamiya, and H. Yanai, "Characteristics of optical guided modes in multilayer metal-clad planar optical guide with low-index dielectric buffer layer," *IEEE J. Quantum Electron.*, vol. QE-11, pp. 729-736, Sept. 1975.

[3] J. N. Polky and G. L. Mitchell, "Metal-clad planar dielectric waveguide for integrated optics," *J. Opt. Soc. Amer.*, vol. 64, pp. 274-279, Mar. 1974.

[4] S. C. Rashleigh, "Four-layer metal-clad thin film optical waveguides," *Opt. and Quantum Electron.*, vol. 8, pp. 49-60, Jan. 1976.

[5] I. P. Kaminow, W. L. Mammel, and H. P. Weber, "Metal-clad optical waveguides: Analytical and experimental study," *Appl. Opt.*, vol. 13, pp. 396-405, Feb. 1974.

[6] Y. Takano and J. Hamasaki, "Propagating modes of a metal-clad dielectric-slab waveguide for integrated optics," *IEEE J. Quantum Electron.*, vol. QE-8, pp. 206-212, Feb. 1972.

[7] Y. Suematsu *et al.*, "Fundamental transverse electric field (TE_0) mode selection in thin-film asymmetric light guide," *Appl. Phys. Lett.*, vol. 21, pp. 291-293, Sept. 1972.

[8] T. E. Batchman and S. C. Rashleigh, "Mode-selective properties of a metal-clad dielectric-slab waveguide for integrated optics," *IEEE J. Quantum Electron.*, vol. QE-8, pp. 848-850, Nov. 1972.

[9] E. M. Garmire and H. Stoll, "Propagation losses in metal-film-substrate optical waveguides," *IEEE J. Quantum Electron.*, vol. QE-8, pp. 763-766, Oct. 1972.

[10] Y. Yamamoto, T. Kamiya, and H. Yanai, "Propagation characteristics of a partially metal-clad optical guide: Metal clad optical stripline," *Appl. Opt.*, vol. 14, p. 322, Feb. 1975.

[11] K. H. Rollke and W. Sohler, "Metal clad waveguide as cutoff polarizer for integrated optics," *IEEE J. Quantum Electron.*, vol. QE-13, pp. 141-145, Apr. 1977.

[12] T. E. Batchman and K. A. McMillan, "Measurement on positive-permittivity metal-clad waveguides," *IEEE J. Quantum Electron.*, vol. QE-13, pp. 187-192, Apr. 1977.

[13] T. E. Batchman and J. R. Peeler, "Gallium arsenide clad optical waveguides," *IEEE J. Quantum Electron.*, vol. QE-14, pp. 327-329, May 1978.

[14] C. M. Lee, P. S. Mak, and A. P. DeFonzo, "Optical control of millimeter-wave propagation in dielectric waveguides," *IEEE J. Quantum Electron.*, vol. QE-16, Mar. 1980.

[15] D. E. Gray, Ed., *American Institute of Physics Handbook*, 2nd ed. New York: McGraw-Hill, 1963, ch. 6, pp. 103-122.

[16] M. H. Brodsky, Ed., "Amorphous semiconductors," in *Topics in Applied Physics*, vol. 36. New York: Springer-Verlag, 1979, pp. 1-7.

[17] R. Fischer, "Luminescence in amorphous semiconductors," in *Amorphous Semiconductors, Topics in Applied Physics*, vol. 36. New York: Springer-Verlag, 1979, pp. 176-180.

[18] R. G. Smith and G. C. Mitchell, "Calculation of complex propagating modes in arbitrary plane-layered complex dielectric structures," Univ. of Washington, Seattle, EE Tech. Rep. 206, Nat. Sci. Foundation Grant Eng. 76-09937, Dec. 1977.

[19] D. E. Carson, "Photo voltaics V: Amorphous silicon cells," *IEEE Spectrum*, pp. 39-41, Feb. 1980.

[20] D. E. Ackley and J. Tauc, "Silicon films as selective absorbers for solar energy conversion," *Appl. Opt.*, vol. 16, pp. 2806-2809, Nov. 1977.

[21] O. S. Heavens, *Optical Properties of Thin Solid Films*. New York: Academic, 1955, pp. 170-172.

[22] J. D. Stratton, *Electromagnetic Theory*. New York: McGraw-Hill, 1941, pp. 515-516.

[23] A. L. Jones, "Coupling of optical fibers and scattering in fibers," *J. Opt. Soc. Amer.*, vol. 55, pp. 261-271, Mar. 1965.

[24] T. K. Lim, B. K. Garside, and J. P. Marton, "An analysis of optical waveguide tapers," *Appl. Phys.*, vol. 18, pp. 53-62, Jan. 1979.

[25] R. B. Smith, "Analytic solutions for linearly tapered directional couplers," *J. Opt. Soc. Amer.*, vol. 66, pp. 882-892, Sept. 1976.

[26] D. P. Gia Russo and J. H. Harris, "Electrooptic modulation in a thin film waveguide," *Appl. Opt.*, vol. 10, pp. 2786-2788, Dec. 1971.

[27] W.S.C. Chang and K. W. Loh, "Theoretical design of guided wave structure for electrooptical modulation at 10.6 μm," *IEEE J. Quantum Electron.*, vol. QE-8, pp. 463-470, June 1972.

[28] J. M. Hammer, R. S. Bartolini, A. Miller, and C. C. Neil, "Optical grating coupling between low index fibers and high index film waveguides," *Appl. Phys. Lett.*, vol. 28, pp. 192-193, Feb. 1976.

[29] D. G. Dalgoutte, R. B. Smith, G. Achutaramayya, and J. H. Harris, "Externally mounted fibers for integrated optics interconnections," *Appl. Opt.*, vol. 14, pp. 1860-1865, Aug. 1975.

T. E. Batchman (S'61-M'66) was born in Great Bend, KS, on March 29, 1940. He received the B.S.E.E., M.S.E.E., and Ph.D. degrees in electrical engineering from the University of Kansas, Lawrence, in 1962, 1963, and 1966, respectively.

From 1966 to 1970 he was an Engineering Scientific Specialist with LTV Missiles and Space Division. In 1970 he joined the faculty of the University of Queensland, Brisbane, Australia, as a Senior Lecturer. Among his research activities at the University of Queensland were integrated optics and dynamic modeling of telecommunications systems. Since 1975 he has been on the faculty of the Department of Electrical Engineering at the University of Virginia, Charlottesville, where he is an Associate Professor. His current research activities include integrated optical devices and microwave sensors.

Dr. Batchman is a member of Eta Kappa Nu, Sigma Tau, Tau Beta Pi, and Sigma Xi.

Glen M. McWright (S'81) was born in Washington, DC, on July 6, 1958. He received the B.S. and M.E. degrees in electrical engineering from the University of Virginia, Charlottesville, in 1980 and 1981, respectively.

He is currently pursuing the Ph.D. degree, also at the University of Virginia.